

# Non-Gaussian Chance-Constrained Trajectory Planning for Autonomous Vehicles in the Presence of Uncertain Agents

Allen Wang, Ashkan Jasour, and Brian C. Williams

**Abstract**—Agent behavior is arguably the greatest source of uncertainty in trajectory planning for autonomous vehicles. This problem has motivated significant amounts of work in the behavior prediction community on learning rich distributions of the future states and actions of agents. However, most current work on trajectory planning in the presence of uncertain agents or obstacles is limited to the case of Gaussian uncertainty with linear constraints, which is a limited representation, or requires sampling, which can be computationally intractable to encode in an optimization problem. In this paper, we present a general method for enforcing chance-constraints on the probability of collision with other agents in trajectory planning problems for autonomous driving that can be used with non-Gaussian mixture models of agent positions. Our method involves using statistical moments of the non-Gaussian distributions in concentration inequalities to upper bound the probability of polynomial constraint violation. In experiments, we show that the resulting optimization problem can be solved with state-of-the-art nonlinear program (NLP) solvers to plan trajectories with 5 second horizons with low latency.

## I. INTRODUCTION

In order for autonomous vehicles to drive safely on public roads, they need to plan trajectories that take into account predictions of future positions of other agents (e.g. human driven vehicles, pedestrians, cyclists). However, predictions are inherently uncertain, especially predictions of human behavior. This fact is motivating significant amounts of work in the behavior prediction community to develop methods that predict *distributions* of future agent states and actions, usually using a deep neural network (DNN). For example, [1] trains a conditional variational autoencoder (CVAE) to generate samples of possible future trajectories; the DNN in this case essentially becomes the distribution from which samples can be drawn. [2], [3] learn Gaussian mixture models (GMMs) for the agents' future positions to handle both uncertainty in high level decisions, which tends to be multi-modal, and uncertainty in execution, which tends to be continuous.

While work in behavior prediction can now generate rich distributions of future agent states and actions, most current works in chance-constrained trajectory planning only address the unimodal case and additionally either make Gaussian assumptions or require sampling [4]–[8]. We argue that handling non-Gaussian distributions is important because, for example, almost any distribution for agent action propagated through nonlinear dynamics models will result in non-Gaussian position distributions. Gaussians also have unbounded supports; this is unrealistic as the reachable set

of agents is bounded by physical laws in reality. To handle non-Gaussian uncertainty, some prior works take a sampling-based approach [5], [6]. This often makes optimization computationally intractable because thousands of constraints need to be introduced to even enforce chance-constraints on the order of  $10^{-2}$  for any practical problem [5]. To address non-Gaussian uncertainty in obstacle or agent positions without sampling, recent works apply concentration inequalities, but they are currently restricted to linear constraints [9]–[12]. For non-Gaussian uncertainty, sums-of-squares programming has been applied to the problem of trajectory tracking for nonlinear systems and risk assessment in the presence of non-convex obstacles, but current computational limitations restrict it to applications amenable to leveraging offline computation [13]–[16].

In this paper, we present a general chance-constrained trajectory planning formulation for autonomous vehicles that can handle mixtures of non-Gaussian distributions of agent position and, unlike many prior works which make point mass assumptions, accounts for the sizes of the ego vehicle and agents. This is enabled by a general methodology we develop for enforcing non-Gaussian polynomial chance-constraints using concentration inequalities, extending the prior art which can only handle linear constraints. This methodology makes heavy use of symbolic algebra, and we develop and provide a Python package, *AlgebraicMoments*<sup>1</sup>, to simplify it. Given a constraint defined as a polynomial in a random vector, *AlgebraicMoments* can generate closed form expressions in terms of statistical moments of the random vector that upper-bounds the probability of the event. It can even directly generate MATLAB or Python code to compute the risk bound, given the necessary inputs. Since this approach only depends on statistical moments of the distributions, it can apply to a wide range of prediction distributions including non-Gaussian mixture models of future agent positions. In numerical experiments, we show how our formulation, when solved with advanced interior-point methods, can be used to plan trajectories with horizons of 5 seconds with low latency.

## II. REPRESENTATION OF AGENT PREDICTIONS

### A. Assumptions

We assume a behavior prediction system provides the distribution of future positions for an agent over a  $T$  step horizon,  $\mathbf{g}_{1:T}$ , in a fixed frame. The distributions can be

All authors are with the Computer Science and Artificial Intelligence Laboratory, MIT. {allenw, jasour, williams}@mit.edu

<sup>1</sup>The source code with examples can be found at [github.com/allen-adastra/algebraic\\_moments](https://github.com/allen-adastra/algebraic_moments).

either unimodal or a mixture of non-Gaussian random vectors. The distributions  $\mathbf{g}_i = [g_{x_i}, g_{y_i}]^T$  are assumed to be either independent across time in the unimodal case or independent across time conditioned on the discrete mode in the mixture model case. This is a common assumption used in state-of-the-art behavior prediction systems; thus, it does not significantly restrict our method's range of applicability [2], [3], [17]. We also make the additional assumption that the predicted distributions do not change w.r.t. changes in the ego vehicle trajectory, as accounting for the change requires having the behavior prediction system in the planning loop. In practice, it may be more effective to alternate between the motion planner and behavior prediction systems by using planned trajectories in the prediction system to generate a new distribution, but we do not explore this interaction in this paper.

### B. Computing Moments of Distributions

In some cases, the statistical moments of distributions are known in closed form. In other cases, statistical moments of a distribution can be rapidly computed by applying automatic or numerical differentiation to its characteristic function (CF). This is a very general approach to computing moments of distributions as CFs always exist, and, from a more practical standpoint, there are extensive tables of CFs for common distributions [18]. Letting  $X$  denote a random variable and  $\Phi_X(t)$  denote its characteristic function, the  $n_{th}$  moment of  $X$  can be computed by:

$$\mathbb{E}[X^n] = i^{-n} \left[ \frac{d^n}{dt^n} \Phi_X(t) \right]_{t=0} \quad (1)$$

Similarly, moments of a random vector,  $\mathbf{w}$ , can be computed via partial differentiation of its joint characteristic function  $\Phi_{\mathbf{w}}(t)$ , although we note catalogues of CFs are less extensive for multivariate distributions. Alternatively, moments may also be estimated with Monte Carlo type methods; this is useful for approaches where the DNN is a distribution from which sampled trajectories are drawn.

### C. Statistics of Mixture Models

A mixture model is a rich way of expressing multi-modal uncertainty by combining multiple continuous distributions [19]. In this work, we work with random vectors and define random vector mixture models as:

**Definition 1.** An  $n$  component **random vector mixture model**  $\mathbf{w}$  is a random vector with components  $\mathbf{w}_i$  and mixture weights  $w_i$  for  $i = 1, \dots, n$  s.t.  $\sum_{i=1}^n w_i = 1$ . Its pdf  $f_{\mathbf{w}}$  is related to those of its components  $f_{\mathbf{w}_i}$  by:

$$f_{\mathbf{w}}(\cdot) = \sum_{i=1}^n w_i f_{\mathbf{w}_i}(\cdot) \quad (2)$$

A useful property of mixture models is its statistics can be computed in terms of statistics of its components [19]. Proposition 2 states this fact in the general case and only makes the mild assumption that  $g(\cdot)$  is measurable, allowing it to apply to most functions used in practice. As a simple

corollary, by letting  $g(\mathbf{w})$  be some moment of  $\mathbf{w}$ , moments of  $\mathbf{w}$  can be expressed as the weighted sum of the moments of its components.

**Proposition 2.** For any  $n$  component random vector mixture model  $\mathbf{w}$  with components  $\mathbf{w}_i$  with mixture weights  $w_i$  and any measurable function  $g$ , we have that  $\mathbb{E}[g(\mathbf{w})] = \sum_{i=1}^n w_i \mathbb{E}[g(\mathbf{w}_i)]$ .

*Proof.* By the law of the unconscious statistician and the definition of the mixture model pdf:

$$\mathbb{E}[g(\mathbf{w})] = \int g(\mathbf{x}) \sum_{i=1}^n w_i f_{\mathbf{w}_i}(\mathbf{x}) d\mathbf{x} \quad (3)$$

Applying the linearity of expectation we then have:

$$\int g(\mathbf{x}) \sum_{i=1}^n w_i f_{\mathbf{w}_i}(\mathbf{x}) d\mathbf{x} = \sum_{i=1}^n w_i \int g(\mathbf{x}) f_{\mathbf{w}_i}(\mathbf{x}) d\mathbf{x} \quad (4)$$

$$= \sum_{i=1}^n w_i \mathbb{E}[g(\mathbf{w}_i)] \quad (5)$$

□

## III. PROBLEM FORMULATION

### A. Definition of Risk

We define risk in a way that accounts for the size of the agent and ego vehicle. The general idea is to fit circles of radius  $r$  to an agent and constrain the probability that the centers of the circles are inside an appropriately scaled “collision ellipsoid” around the vehicle. Figure 1 illustrates an example; note that if the centers of the circles are not in the ellipsoid, the vehicles are not in collision. We essentially

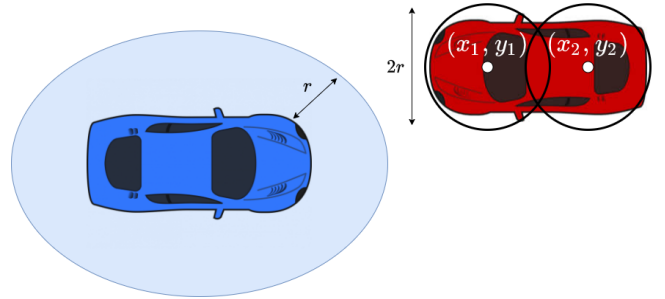


Fig. 1. An example showing a collision ellipsoid around the ego vehicle and corresponding circles around the agent. Note that if the points  $(x_i, y_i)$  are not in the ellipsoid, then the vehicles are not in collision.

treat each circle as a separate agent. We will define risk in the “planned body frames”, which are depicted by figure 2. While the prediction is given in some fixed frame, we eventually show in section IV-D how moments in the planned body frames can be expressed as a function of the fixed frame moments and the planned ego vehicle pose. In the body frame, the ellipsoid is the set:

$$\{\mathbf{x} : \mathbf{x}^T Q \mathbf{x} \leq 1\} \quad (6)$$

Where  $Q$  is a constant  $2 \times 2$  positive definite matrix. The following notation will be used for quadratic forms as it

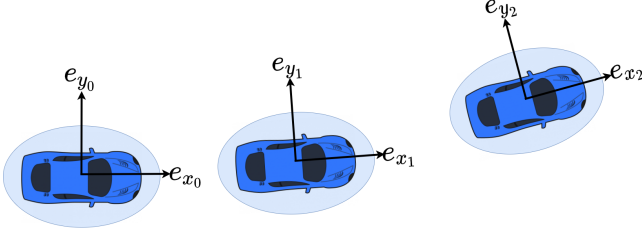


Fig. 2. A planned trajectory for the ego vehicle along with the “planned body frames” and collision ellipsoids drawn around the vehicle.

better reflects the polynomial nature of quadratic forms, and many results in this paper will be for polynomials in general:

$$Q(\mathbf{x}) := \mathbf{x}^T Q \mathbf{x} \quad (7)$$

We denote the distribution of the  $i_{th}$  agent in the planned frame at time  $t$  as  $\mathbf{a}_{t,i}$ ; recall this distribution is ultimately a function of the global frame prediction  $\mathbf{g}_{t,i}$  and the planned ego vehicle pose. Risk along the horizon is thus defined as:

$$\mathcal{R} := \mathbb{P} \left( \bigcup_{i=1}^{n_a} \bigcup_{t=1}^T \{Q(\mathbf{a}_t) \leq 1\} \right) \quad (8)$$

However, evaluating (8) without excessive conservatism is a non-trivial problem itself meriting a separate treatment. For this paper, we simply apply Boole’s Inequality which states:

$$\mathcal{R} \leq \sum_{i=1}^{n_a} \sum_{t=1}^T \mathbb{P}(Q(\mathbf{a}_{t,i}) \leq 1) \quad (9)$$

To upper bound the total risk  $\mathcal{R}$  with some  $\Delta$ , we define a risk-allocation  $\epsilon_{t,i}$  s.t.:

$$\sum_{i=1}^{n_a} \sum_{t=1}^T \epsilon_{t,i} \leq \Delta \quad (10)$$

And then upper-bound the marginal probabilities as such:

$$\mathbb{P}(Q(\mathbf{a}_{t,i}) \leq 1) \leq \epsilon_{t,i} \quad (11)$$

It is possible to encode the risk allocation as decision variables in an optimization problem, but doing so can often be computationally intractable. In this paper, we solve the trajectory planning problem with a fixed risk allocation; other works have presented approaches for “outer loops” that optimize the risk allocation [12], [20], [21]. In addition, throughout the rest of this paper, we present mathematical statements for the single agent case for the sake of notational simplicity; it is straight-forward to simply repeat the chance-constraint in the multi-agent case.

## B. The Trajectory Planning Problem

In this paper, we derive results for the general cc-trajectory planning problem defined below.

$$\min_{\mathbf{x}_{1:T}, \mathbf{u}_{0:T}} c(\mathbf{x}_{1:T}, \mathbf{u}_{1:T}) \quad (12a)$$

$$\mathbf{x}_{t+1} = f(\mathbf{x}_t, \mathbf{u}_t), \quad t \in [T-1] \quad (12b)$$

$$\mathbb{P}(Q(\mathbf{a}_t) \leq 1) \leq \epsilon_t, \quad t \in [T] \quad (12c)$$

$$\mathbf{u}_{min} \leq \mathbf{u}_t \leq \mathbf{u}_{max}, \quad t \in [T] \quad (12d)$$

$$\mathbf{x}_{min} \leq \mathbf{x}_t \leq \mathbf{x}_{max}, \quad t \in [T] \quad (12e)$$

Where  $\mathbf{x}_t$  is the state vector,  $\mathbf{u}_t$  is the control vector,  $c$  is some cost function,  $f$  is a discrete time system modeling ego vehicle dynamics,  $\mathbf{u}_{min}$  and  $\mathbf{u}_{max}$  are control limits and  $\mathbf{x}_{min}$  and  $\mathbf{x}_{max}$  are state limits. We assume that the ego vehicle dynamics are deterministic as modern feedback control systems for autonomous vehicles are effective at tracking trajectories with positional error on the order of ten centimeters [22], [23]. Thus, the only difference between this problem and standard deterministic trajectory planning formulations is the chance constraint (12c) which ensures that the probability of the vehicle colliding with an agent is no more than  $\epsilon$  at each time step. Section IV presents our approach to enforcing a risk-bound on this chance constraint.

## IV. ENFORCING POLYNOMIAL NON-GAUSSIAN CHANCE-CONSTRAINTS

In this section, we present a general methodology for enforcing polynomial non-Gaussian chance-constraints; that is, for a random vector  $\mathbf{w}$  and polynomial  $p$ , we present a method to establish a bound on the probability:

$$\mathbb{P}(p(\mathbf{w}) \leq 0) \quad (13)$$

Recall that the chance-constraint in our trajectory planning problem (12c) takes this form as quadratic forms are polynomials. By viewing  $p(\mathbf{w})$  as a random variable, (13) is simply the cumulative distribution function (cdf) of  $p(\mathbf{w})$  evaluated at 0. Unfortunately, even in the relatively simple case where  $\mathbf{w}$  is a multivariate Gaussian and  $p$  is a quadratic,  $p(\mathbf{w})$  does not have a closed form cdf [24]. In general, it can be very challenging to characterize the cdfs of distributions that arise from nonlinear transformations, so our approach is to leverage one-tailed concentration inequalities which bound (13) using the mean and variance of  $p(\mathbf{w})$ . Subsection IV-A begins by showing how moments of the random variable  $p(\mathbf{w})$  can be expressed in closed form in terms of moments of  $\mathbf{w}$ . This provides us with a way to compute the mean and variance of  $p(\mathbf{w})$  given the distribution of  $\mathbf{w}$ . Subsection IV-B then introduces several concentration inequalities that can be used to bound (13) using the mean and variance of  $p(\mathbf{w})$ . We can directly apply these approaches to mixture models by computing the moments of the mixture models with the approach from subsection II-C. However, we show in subsection IV-C that tighter bounds can be achieved by instead bounding the components of the mixture model. Finally, subsection IV-D applies these techniques to bound the chance-constraint (12c).

### A. Moments of Polynomials in Random Vectors

An important property of  $p$  being a polynomial is that the  $n_{th}$  moment of  $p(\mathbf{w})$  can be computed as the weighted sum of moments of  $\mathbf{w}$ . This is true because  $p(\mathbf{w})^n$  is, itself, a polynomial to which the linearity of expectation can be applied. To see this, consider the following simple example where  $p(\mathbf{w}) = w_1^2 + w_2^2$ :

$$\mathbb{E}[p(\mathbf{w})^2] = \mathbb{E}[w_1^4 + 2w_1^2w_2^2 + w_2^4] \quad (14a)$$

$$= \mathbb{E}[w_1^4] + 2\mathbb{E}[w_1^2w_2^2] + \mathbb{E}[w_2^4] \quad (14b)$$

To state the general case, we adopt multi-index notation which allows us to much more succinctly express moments of random vectors. For example,  $\mathbb{E}[w_1^2w_2^2]$  can be represented with the vector  $\mathbf{w}$  and a multi-index  $\alpha = (2, 2, 0, \dots, 0)$ . Letting  $\mathbf{w}$  be an  $n$  dimensional random vector, we can express any moment of  $\mathbf{w}$  with a multi-index  $\alpha \in \mathbb{N}^n$  as such where  $\alpha_i$  is the  $i_{th}$  element of  $\alpha$ :

$$\mathbb{E}[\mathbf{w}^\alpha] := \mathbb{E}\left[\prod_{i=1}^n w_i^{\alpha_i}\right] \quad (15)$$

Proposition 3 uses multi-index notation to express the idea that any moment of  $p(\mathbf{w})$  can be expressed in terms of moments of  $\mathbf{w}$ . AlgebraicMoments can be used to easily derive expressions of the form (16), and it even leverages independence in the random vector  $\mathbf{w}$  to further decompose terms of the form  $\mathbb{E}[\mathbf{w}^\alpha]$ .

**Proposition 3.** *For a  $n$  dimensional random vector  $\mathbf{w}$ , a polynomial  $p$  and  $m \in \mathbb{N}$ , there exists a set of multi-indices  $\mathcal{A} \subset \mathbb{N}^n$  and coefficients  $C_{\mathcal{A}} = \{c_\alpha \in \mathbb{R} : \alpha \in \mathcal{A}\}$  s.t.:*

$$\mathbb{E}[p(\mathbf{w})^m] = \sum_{\alpha \in \mathcal{A}} c_\alpha \mathbb{E}[\mathbf{w}^\alpha] \quad (16)$$

*Proof.* Since  $p$  is a polynomial,  $p(\mathbf{w})^m$  is also a polynomial in  $\mathbf{w}$  since the ring of polynomials is closed under multiplication. Thus, we have the existence of  $\mathcal{A}$  and  $C_{\mathcal{A}}$  s.t.  $p(\mathbf{w})^m = \sum_{\alpha \in \mathcal{A}} c_\alpha \mathbf{w}^\alpha$ . Applying the expectation operator to both sides and the linearity of expectation, we arrive at the result.  $\square$

### B. Bounding Risk with Concentration Inequalities

The prior subsection shows how moments of  $p(\mathbf{w})$  can be expressed in terms of moments of  $\mathbf{w}$ ; in this section we show how the mean and variance of  $p(\mathbf{w})$ ,  $\mu_{p(\mathbf{w})}$  and  $\sigma_{p(\mathbf{w})}^2$ , can be used to bound risk using concentration inequalities. We start with Cantelli's inequality [25], also known as the one-tailed Chebyshev Inequality, which bounds the probability of constraint violation as such:

$$\mathbb{P}(p(\mathbf{w}) \leq 0) \begin{cases} \leq \frac{\sigma_{p(\mathbf{w})}^2}{\sigma_{p(\mathbf{w})}^2 + \mu_{p(\mathbf{w})}^2} & \mu_{p(\mathbf{w})} \geq 0 \\ \geq 1 - \frac{\sigma_{p(\mathbf{w})}^2}{\sigma_{p(\mathbf{w})}^2 + \mu_{p(\mathbf{w})}^2} & \mu_{p(\mathbf{w})} < 0 \end{cases} \quad (17)$$

However, for many applications, Cantelli's inequality can be excessively conservative; in fact, it is often sharp only for discrete distributions. By making additional mild assumptions, we can arrive at tighter bounds with the Vysochanskij-Petunin (VP) and Gauss inequalities, which are very similar

[26]. Our proposed strategy is to adopt the tightest inequality for which  $p(\mathbf{w})$  meets the given assumptions; the table below summarizes the assumptions for each inequality. Since the

Inequality	Assumptions
Cantelli	$p(\mathbf{w})$ has finite mean + variance
Vysochanskij-Petunin (VP)	Cantelli assumptions + unimodal
Gauss	VP assumptions + symmetric pdf

TABLE I

ASSUMPTIONS REQUIRED FOR CONCENTRATION INEQUALITIES.

inequalities are very similar, we simplify future notation by defining the  $\text{Conc}[\cdot]$  operator to denote the tightest appropriate concentration inequality and  $\text{Conc}^*[\cdot]$  to denote the corresponding necessary condition for the inequality to hold. In practice, the practitioner would have to select the correct inequality to use on a case-by-case basis.

$$\text{Conc}[p(\mathbf{w})] = \begin{cases} \frac{\sigma_{p(\mathbf{w})}^2}{\sigma_{p(\mathbf{w})}^2 + \mu_{p(\mathbf{w})}^2} & \text{Cantelli Holds} \\ \frac{4}{9} \frac{\sigma_{p(\mathbf{w})}^2}{\sigma_{p(\mathbf{w})}^2 + \mu_{p(\mathbf{w})}^2} & \text{VP Holds} \\ \frac{2}{9} \frac{\sigma_{p(\mathbf{w})}^2}{\mu_{p(\mathbf{w})}^2} & \text{Gauss Holds} \end{cases} \quad (18)$$

$$\text{Conc}^*[p(\mathbf{w})] = \begin{cases} -\mu_{p(\mathbf{w})} & \text{Cantelli Holds} \\ -\mu_{p(\mathbf{w})} + \sqrt{\frac{5}{3}} \sigma_{p(\mathbf{w})} & \text{VP Holds} \\ -\mu_{p(\mathbf{w})} + \frac{2}{3} \sigma_{p(\mathbf{w})} & \text{Gauss Holds} \end{cases} \quad (19)$$

Thus, an  $\epsilon$  chance-constrain can be enforced in an optimization problem by enforcing the constraints:

$$\text{Conc}[p(\mathbf{w})] \leq \epsilon \quad (20)$$

$$\text{Conc}^*[p(\mathbf{w})] \leq 0 \quad (21)$$

Note that the  $\text{Conc}^*$  conditions are not particularly restrictive, as they are only violated when risk is relatively high. In fact, the  $\text{Conc}^*$  condition only breaks when the upper-bound is at least 1, 1/6, or 1/2 for the Cantelli, VP, and Gauss cases respectively, which is well above values usually specified for chance-constraints in practice.

### C. Tighter Bounds for Mixture Models

In the case that  $\mathbf{w}$  is a mixture model we can simply compute the moments of  $p(\mathbf{w})$  using the result of proposition 2 in terms of moments of the components  $p(\mathbf{w}_i)$  and treat the mixture model as any other random variable. However, proposition 2 also seems to suggest that we can instead bound the component probabilities  $\mathbb{P}(p(\mathbf{w}_i) \leq 0)$  and bound the overall risk with the weighted sum of the component bounds. Intuition indicates this approach to be better because it involves applying concentration inequalities at the most detailed level possible. Since concentration inequalities are essentially blanket statements about a distribution, it makes sense to apply them at the most detailed level possible. In fact, we show with theorem 4 that applying concentration inequalities to the mixture components individually will almost certainly produce a less conservative risk bound.

**Theorem 4.** For any random vector mixture model  $\mathbf{w}$  with  $n$  components  $\mathbf{w}_i$  and weights  $w_i$  and any measurable function  $g$ , if  $\text{Conc}^*[g(\mathbf{w}_i)] \leq 0, \forall i \in [n]$ , then:

$$\mathbb{P}(g(\mathbf{w}) \leq 0) \leq \sum_{i=1}^n w_i \text{Conc}(g(\mathbf{w}_i)) \quad (22a)$$

$$\leq \text{Conc}(g(\mathbf{w})) \quad (22b)$$

For Cantelli and VP, almost surely, we have:

$$\sum_{i=1}^n w_i \text{Conc}(g(\mathbf{w}_i)) < \text{Conc}(g(\mathbf{w})) \quad (23)$$

*Proof.* See appendix.  $\square$

**Remark 1.** “Almost surely” in theorem 4 means that if the first and second moments of each component are randomly chosen from  $\mathbb{R}^2$  according to any distribution supported on a subset of  $\mathbb{R}^2$  with non-zero Lebesgue measure, then the result holds with probability one.

#### D. Bounding Risk for Our Problem

We now return to the problem of establishing a bound on:

$$\mathbb{P}(Q(\mathbf{a}_t) \leq 1) \quad (24)$$

Letting  $\mathbf{a}_t^{(i)}$  denote the  $i_{th}$  component of  $\mathbf{a}_t$ , this essentially consists of applying the methods of the prior subsections to the polynomial  $Q(\mathbf{a}_t^{(i)}) - 1$ . However, there is one small additional complication:  $\mathbf{a}_t^{(i)}$  is in the body frame and is a function of the planned ego vehicle pose and the  $i_{th}$  component of the global frame distribution  $\mathbf{g}_t^{(i)}$ . Letting  $\mathbf{y}_t = [x_t, y_t]$  denote the ego vehicle position,  $\theta_t$  denote the ego vehicle heading, and  $R(\cdot)$  denote the 2D rotation matrix, they are related by:

$$\mathbf{a}_t^{(i)} = R(\theta_t)^T (\mathbf{g}_t^{(i)} - \mathbf{y}_t) \quad (25)$$

The idea here is to view  $\mathbf{a}_t^{(i)}$  as a polynomial in  $\mathbf{g}_t^{(i)}$  and to view the elements of both  $R(\theta_t)^T$  and  $\mathbf{y}_t$  as elements of the coefficients. From this perspective, we apply AlgebraicMoments to express moments of  $\mathbf{a}_t^{(i)}$  in terms of moments of  $\mathbf{g}_t^{(i)}$ . The moments of  $Q(\mathbf{a}_t^{(i)}) - 1$  can, in turn, be expressed in terms of the moments of  $\mathbf{a}_t^{(i)}$ . With the first and second moments of  $Q(\mathbf{a}_t^{(i)}) - 1$  expressed in closed form, we can enforce the following constraints in the optimization problem where  $n$  is the number of mixture components:

$$\sum_{i=1}^n \text{Conc}[Q(\mathbf{a}_t^{(i)}) - 1] \leq \epsilon_t, \quad t \in [T] \quad (26)$$

$$\text{Conc}^*[Q(\mathbf{a}_t^{(i)}) - 1] \leq 0, \quad i \in [n] \quad t \in [T] \quad (27)$$

Since  $Q(\mathbf{a}_t^{(i)}) - 1 \geq 0$ , only the Cantelli and VP inequalities can be used for this particular problem when the support of  $Q(\mathbf{a}_t^{(i)}) - 1$  is unbounded as the Gauss inequality requires symmetry of the pdf.

## V. APPLICATION TO TRAJECTORY PLANNING WITH MODEL PREDICTIVE CONTOURING CONTROL

In the context of autonomous driving, an approximate coarse-grained path is almost always available to trajectory planners as most autonomous driving systems have maps of lane geometries *a priori* and also have routers and higher level planners that provide a discrete plan (e.g: a sequence of waypoints along the road). This availability of a “reference path” makes model predictive contouring control (MPCC) a useful approach. MPCC is a methodology for expressing an approximation of the minimum distance from a point to a third order polynomial in closed form. This allows for deviations from the reference path to be included in the cost function of an optimization problem. By jointly applying MPCC and our chance-constraint formulation, we arrive at a trajectory planner that can find trajectories with low deviation from the reference path while satisfying some desired level of safety, allowing for the generation of rich qualitative behavior. In the following subsections, we present a brief overview of the MPCC formulation; the interested reader is referred to [4], [27] for additional details.

#### A. Reference Path

Following the standard contouring control formulation, the reference path is represented as third order polynomials in an arc-length parameter  $s \in [0, L]$  where  $L$  is the length:

$$\begin{bmatrix} x_{ref}(s) \\ y_{ref}(s) \end{bmatrix} = \begin{bmatrix} c_{x0} + c_{x1}s + c_{x2}s^2 + c_{x3}s^3 \\ c_{y0} + c_{y1}s + c_{y2}s^2 + c_{y3}s^3 \end{bmatrix} \quad (28)$$

Where  $c_{xi}$  and  $c_{yi}$  for  $i \in [3]$  are the polynomial coefficients. Parameterizing a third order polynomial path with arc-length is a difficult problem itself without exact solutions, but approximation methods are well-studied [28], [29]. For our experiments, we applied a simple approximation by initially generating the polynomials with  $s \in [0, 1]$  and then the lengths of the polynomials were computed by numerical integration. The coefficients are then scaled s.t.  $s \in [0, L]$ . The heading at each point on the reference path, denote it  $\Theta(s)$ , can be expressed as such:

$$\Theta(s) = \arctan \left( \frac{\partial y_{ref}}{\partial x_{ref}}(s) \right) \quad (29)$$

#### B. Contouring Deviation and Lag Error

Ideally, the Euclidean distance from the ego vehicle to the nearest point on the reference path, which we will refer to as *contouring deviation*<sup>2</sup>, would be used as the measure of deviation from the reference path, but doing so requires a minimization over the path parameter  $s$  that is computationally intractable to perform in an optimization routine. The standard solution is to approximate the contouring deviation by using the distance the vehicle has travelled, denote it  $\Delta$ , as an approximation. This only requires adding an additional integrator variable to the dynamics model as

<sup>2</sup>In the literature, this is usually known as *contouring error*, but we call it contouring deviation as deviation from the reference path to satisfy chance-constraints is not necessarily undesirable.

the time derivative of  $\Delta$  is the vehicles speed. Letting  $\bar{x}_t = x_t - x_{ref}(\Delta_t)$  and  $\bar{y}_t = y_t - y_{ref}(\Delta_t)$ , contouring deviation can be approximated with:

$$D_t = \sin(\Theta(\Delta_t))\bar{x}_t - \cos(\Theta(\Delta_t))\bar{y}_t \quad (30)$$

It is also important to penalize error between  $\Delta$  and the true parameter corresponding to the closest point on the path to the vehicle. This quantity is known as the *lag error* and can be approximated by:

$$L_t = -\cos(\Theta(\Delta_t))\bar{x}_t - \sin(\Theta(\Delta_t))\bar{y}_t \quad (31)$$

### C. Ego Vehicle Model

For driving in nominal conditions, the kinematic bicycle model is known to provide a high level of fidelity while requiring less computational cost than a dynamics model making it well suited for trajectory planning [30]. The state of the vehicle is defined as  $\mathbf{x} = [x, y, \theta, v, \delta, \Delta]^T$  where  $x, y$  denotes the vehicle's position and  $\theta$  denotes the heading in the global coordinates.  $v$  denotes speed,  $\delta$  denotes the front steering angle, and  $\Delta$  denotes the distance traveled. The control inputs are  $\mathbf{u} = [u_a, u_\delta]^T$  where  $u_a$  is acceleration and  $u_\delta$  is the rate of change of the steering angle. The relevant physical parameters of the vehicle in this model are the distances from the center of gravity to the front and rear axles; we denote them  $l_f$  and  $l_r$  respectively. The continuous time model is thus:

$$\dot{\mathbf{x}} = \begin{bmatrix} v \cos(\theta + \beta) \\ v \sin(\theta + \beta) \\ \frac{v}{l_r} \sin(\beta) \\ u_a \\ u_\delta \\ v \end{bmatrix} \quad \beta = \arctan\left(\frac{l_r}{l_f + l_r} \tan(\delta)\right) \quad (32)$$

### D. Optimization Statement

In the cost function, we penalize contouring deviation, lag error, control effort, and deviation from a reference speed (e.g: the roads speed limit):

$$c(\mathbf{x}_t, \mathbf{u}_t) = c_D D_t^2 + c_L L_t^2 + \mathbf{u}_t^T R \mathbf{u}_t + c_v (v_t - v^*)^2 \quad (33)$$

Where  $c_D, c_L, c_v \in \mathbb{R}$  and  $R \in \mathcal{S}_{++}^2$  are cost function parameters and  $v^*$  is the reference speed. Letting  $f_{RK4}$  denote the RK4 approximation of the bicycle model, the full problem we solve is:

$$\min \sum_{t=0}^T c(\mathbf{x}_t, \mathbf{u}_t) \quad (34a)$$

$$\mathbf{x}_{t+1} = f_{RK4}(\mathbf{x}_t, \mathbf{u}_t), \quad t \in [T-1] \quad (34b)$$

$$\sum_{i=1}^n \text{Conc}[Q(\mathbf{a}_t^{(i)}) - 1] \leq \epsilon_t, \quad t \in [T] \quad (34c)$$

$$\text{Conc}^*[Q(\mathbf{a}_t^{(i)}) - 1] \leq 0, \quad i \in [n] \quad t \in [T] \quad (34d)$$

$$\mathbf{x}_{min} \leq \mathbf{x}_t \leq \mathbf{x}_{max}, \quad t \in [T] \quad (34e)$$

$$\mathbf{u}_{min} \leq \mathbf{u}_t \leq \mathbf{u}_{max}, \quad t \in [T-1] \quad (34f)$$

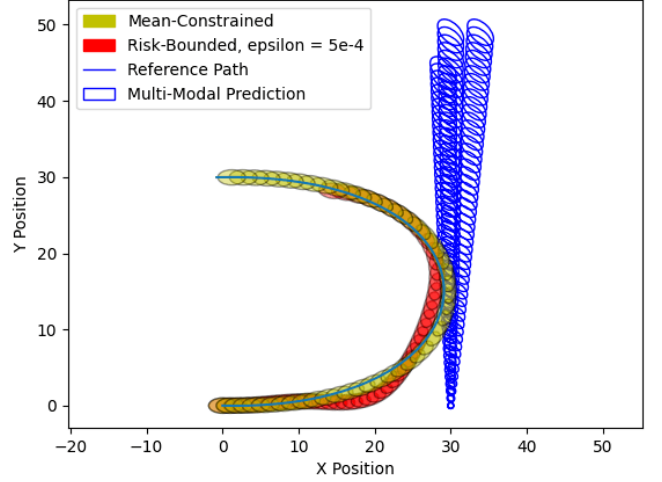


Fig. 3. Comparison between trajectories planned with a deterministic mean-constrained formulation and the risk-bounded formulation. The risk-bounded formulation exhibits noticeably more cautious behavior when performing the U-turn, by taking a wider and slower turn.

## VI. NUMERICAL EXPERIMENTS

For numerical experiments, we used optimizers generated with FORCES Pro, a software package that generates high performance interior-point solvers for optimal control problems that exploit structure induced in the Karush-Kuhn-Tucker (KKT) system by the step-wise nature of optimal control problems [31], [32]. A third order polynomial path emulating a U-turn was generated to serve as the reference path. Example non-Gaussian mixture-model behavior predictions were created by manually specifying mean vectors and covariance matrices, computing the higher order moments corresponding to multivariate Gaussians with these parameters, and then perturbing the higher order moments. 50 time steps were used with intervals of 0.1 seconds for a planning horizon of 5 seconds. Initial guesses for the optimizer were produced by simulating the system (34c) with constant control inputs.

Figure 3 shows two trajectories planned with two different formulations: one deterministic and the other risk-bounded. The deterministic formulation involved using the means of the agent predictions to enforce the collision constraint. The risk-bounded formulation set  $\epsilon = 0.0005$  and utilized the VP inequality. Note how the risk-bounded formulation plans a qualitatively more cautious trajectory, by taking a wider turn at a slower speed. To test the reliability of the planner, the parameters of the reference path were perturbed to generate 1000 different paths. The trajectory planner was tested on all 1000 paths with a risk bound of 0.0005. 999 of the trials successfully achieved a local optima with a mean solve time of 12.6 ms and a worst case solve time of 26.1 ms with the KKT conditions satisfied within numerical tolerances.

## VII. CONCLUSIONS

In this paper, we presented a chance-constrained trajectory planning formulation for autonomous vehicles that can handle mixtures of non-Gaussian distributions of agent positions



and does not need to make point mass assumptions. To enforce the chance-constraint, we present a general framework that leverages symbolic algebra to generate expressions that upper-bound polynomial chance-constraints in terms of statistical moments of the underlying distribution. We demonstrated this approach by planning trajectories in the presence of uncertain agents in numerical experiments and show the optimization problem can be run with low latency. We also provide a Python package “AlgebraicMoments” to enable other members of the community to adopt our approach to bounding chance-constraints. We note that while enforcing chance-constraints using the presented concentration inequalities provides great generality, this generality can also produce excessively conservative results. Future works should consider leveraging higher order moments, or other distribution specific information, to establish tighter bounds.

#### ACKNOWLEDGEMENTS

This work was supported in part by the Masdar Institute grant 6938857. Allen Wang was supported in part by an NSF Graduate Research Fellowship. The authors would also like to acknowledge the generosity of Embotech for supplying academic FORCES Pro licenses.

#### VIII. APPENDIX

**Lemma 5.** *The function  $\phi(x, y) = \frac{x^2}{y}$  on the domain  $x \in \mathbb{R}$  and  $y > 0$  is convex.*

*Proof.* It is sufficient for the Hessian of  $\phi$  to be positive semi-definite (psd). The eigenvalues of the Hessian can be found in closed form with symbolic algebra:

$$\lambda_1 = 0 \quad \lambda_2 = 2(x^2 + y^2)y^{-3} \quad (35)$$

Since  $y > 0$  on the domain of  $\phi$ , both eigenvalues are non-negative, so the Hessian is psd on the domain of  $\phi$ .  $\square$

##### A. Proof of Theorem 4

*Proof.* We begin by showing the inequality (22a). The probability of constraint violation can be written as the expectation of the indicator function. Define the indicator function:

$$\mathbb{1}_{(-\infty, 0]}(x) = \begin{cases} 1 & x \in (-\infty, 0] \\ 0 & o.w. \end{cases} \quad (36)$$

The probability can then be expressed as:

$$\mathbb{P}(g(\mathbf{w}) \leq 0) = \mathbb{E}[\mathbb{1}_{(-\infty, 0]}(g(\mathbf{w}))] \quad (37)$$

The indicator function (36) is measurable [33], so we can apply proposition 2:

$$\mathbb{E}[\mathbb{1}_{(-\infty, 0]}(g(\mathbf{w}))] = \sum_{i=1}^n w_i \mathbb{P}(g(\mathbf{w}_i) \leq 0) \quad (38)$$

$$\leq \sum_{i=1}^n w_i \text{Conc}[g(\mathbf{w}_i)] \quad (39)$$

Now, we show the inequality (22b) for the Cantelli and VP cases. Since VP is just a constant scaling of Cantelli, the results for Cantelli apply directly to VP. We rewrite:

$$\frac{\text{Var}[g(\mathbf{w})]}{\text{Var}[g(\mathbf{w})] + \mathbb{E}[g(\mathbf{w})^2]} = 1 - \frac{\mu_{g(\mathbf{w})}}{\mathbb{E}[g(\mathbf{w})^2]} \quad (40)$$

$$= 1 - \phi(\mu_{g(\mathbf{w})}, \mathbb{E}[g(\mathbf{w})^2]) \quad (41)$$

By Lemma 5,  $\phi$  above is convex since  $\mathbb{E}[g(\mathbf{w})^2] > 0$ <sup>3</sup>. By decomposing the moments we have:

$$\left[ \frac{\mu_{g(\mathbf{w})}}{\mathbb{E}[g(\mathbf{w})^2]} \right] = \sum_{i=1}^n w_i \left[ \frac{\mu_{g(\mathbf{w}_i)}}{\mathbb{E}[g(\mathbf{w}_i)^2]} \right] \quad (42)$$

Thus, by the finite version of Jensen’s inequality:

$$\phi(\mu_{g(\mathbf{w})}, \mathbb{E}[g(\mathbf{w})^2]) \leq \sum_{i=1}^n w_i \phi(\mu_{g(\mathbf{w}_i)}, \mathbb{E}[g(\mathbf{w}_i)^2]) \quad (43)$$

Subtracting the left hand side quantity from 1 and the right hand side quantity from  $\sum_{i=1}^n w_i = 1$ , we have:

$$\text{Conc}[g(\mathbf{w})] \geq \sum_{i=1}^n w_i (1 - \phi(\mu_{g(\mathbf{w}_i)}, \mathbb{E}[g(\mathbf{w}_i)^2])) \quad (44)$$

$$= \sum_{i=1}^n w_i \text{Conc}[g(\mathbf{w}_i)] \quad (45)$$

The exact same argument can be applied to the Gauss inequality by establishing convexity of:

$$\text{Var}[g(\mathbf{w}_i)] / \mu_{g(\mathbf{w}_i)}^2 \quad (46)$$

on the domain with  $\text{Var}[g(\mathbf{w}_i)] > 0$ . We now turn our attention to establishing almost sure strictness of the inequality. It will be sufficient to show that Jensen’s inequality is strict. Jensen’s inequality is strict if  $\phi$  is strictly convex. The key idea is that  $\phi$  is indeed strictly convex if we further restrict its domain by removing a set of Lebesgue measure zero. Recall from Lemma 5 that on the domain  $D$  of  $\phi$ , the eigenvalue  $\lambda_2$  is strictly positive, but  $\lambda_1 = 0$ . Thus, if we restrict the domain of  $\phi$  to not contain the eigenspace of  $\lambda_1 = 0$  for each component, denote this restricted domain  $\hat{D}$ , then we have that  $\phi$  is strictly convex on  $\hat{D}$ . This set  $\hat{D}$  is characterized in terms of moments of components of  $g(\mathbf{w})$ . The eigenspace for the  $i_{th}$  component,  $\hat{D}_i$  is:

$$\mathbf{u}_i := \left[ \frac{\mu_{g(\mathbf{w}_i)}}{\mathbb{E}[g(\mathbf{w}_i)^2]}, 1 \right]^T \quad \hat{D}_i := \{\alpha \mathbf{u}_i : \alpha \in \mathbb{R}\} \quad (47)$$

We arrive at  $\hat{D}$  by removing the union of  $\hat{D}_i$ :

$$\hat{D} := D - \cup_{i=1}^n \hat{D}_i \quad (48)$$

Note that  $\cup_{i=1}^n \hat{D}_i$  is the union of lines and, thus, has Lebesgue measure zero. One complication is that  $[\mu_{g(\mathbf{w}_i)}, \mathbb{E}[g(\mathbf{w}_i)^2]]^T$  does lie on  $\hat{D}_i$ , but it will be sufficient for it to not lie on any other  $\hat{D}_i$ ; that is, we require:

$$\forall i \in [n], \quad [\mu_{g(\mathbf{w}_i)}, \mathbb{E}[g(\mathbf{w}_i)^2]]^T \notin \cup_{j \in [n], j \neq i} \hat{D}_j \quad (49)$$

<sup>3</sup>Technically, it is possible for the second moment to be zero when the random variable is zero with probability one, but this is a pathological case that should never be encountered in practice.

By requiring the first and second moments of each component to not lie on any  $\hat{D}_i$  line corresponding to other components, we require Jensen's inequality to cross the interior of the set on which  $\phi$  is strictly convex. By the analytic statement of Jensen's Inequality under strict convexity [34], we thus have that under the conditions  $w_i > 0$  and  $[\mu_{g(\mathbf{w}_i)}, \mathbb{E}[g(\mathbf{w}_i)^2]]^T$  are unique  $\forall i \in [n]$ :

$$\phi(\mu_{g(\mathbf{w})}, \mathbb{E}[g(\mathbf{w})^2]) < \sum_{i=1}^n w_i \phi(\mu_{g(\mathbf{w}_i)}, \mathbb{E}[g(\mathbf{w}_i)^2]) \quad (50)$$

Since the set  $\bigcup_{i=1}^n \hat{D}_i$  has measure zero, if we choose first and second moment pairs at random according to any distribution supported on some subset of  $\mathbb{R}^2$  with non-zero Lebesgue measure, the probability of the components not satisfying the condition (49) is zero.  $\square$

## REFERENCES

- [1] N. Lee, W. Choi, P. Vernaza, C. B. Choy, P. H. Torr, and M. Chandraker, "Desire: Distant future prediction in dynamic scenes with interacting agents," in *Proceedings of the IEEE Conference on Computer Vision and Pattern Recognition*, 2017, pp. 336–345.
- [2] Y. Chai, B. Sapp, M. Bansal, and D. Anguelov, "Multipath: Multiple probabilistic anchor trajectory hypotheses for behavior prediction," *arXiv preprint arXiv:1910.05449*, 2019.
- [3] N. Deo and M. M. Trivedi, "Multi-modal trajectory prediction of surrounding vehicles with maneuver based lstms," in *2018 IEEE Intelligent Vehicles Symposium (IV)*. IEEE, 2018, pp. 1179–1184.
- [4] W. Schwarting, J. Alonso-Mora, L. Pauli, S. Karaman, and D. Rus, "Parallel autonomy in automated vehicles: Safe motion generation with minimal intervention," in *2017 IEEE International Conference on Robotics and Automation (ICRA)*. IEEE, 2017, pp. 1928–1935.
- [5] G. C. Calafiore and M. C. Campi, "The scenario approach to robust control design," *IEEE Transactions on automatic control*, vol. 51, no. 5, pp. 742–753, 2006.
- [6] L. Blackmore, M. Ono, A. Bektassov, and B. C. Williams, "A probabilistic particle-control approximation of chance-constrained stochastic predictive control," *IEEE transactions on Robotics*, vol. 26, no. 3, pp. 502–517, 2010.
- [7] L. Blackmore and M. Ono, "Convex chance constrained predictive control without sampling," in *AIAA Guidance, Navigation, and Control Conference*, 2009, p. 5876.
- [8] B. Luders, M. Kothari, and J. How, "Chance constrained rrt for probabilistic robustness to environmental uncertainty," in *AIAA guidance, navigation, and control conference*, 2010, p. 8160.
- [9] T. Summers, "Distributionally robust sampling-based motion planning under uncertainty," in *2018 IEEE/RSJ International Conference on Intelligent Robots and Systems (IROS)*. IEEE, 2018, pp. 6518–6523.
- [10] V. Renganathan, I. Shames, and T. H. Summers, "Towards integrated perception and motion planning with distributionally robust risk constraints," *arXiv preprint arXiv:2002.02928*, 2020.
- [11] A. Mesbah, "Stochastic model predictive control: An overview and perspectives for future research," *IEEE Control Systems Magazine*, vol. 36, no. 6, pp. 30–44, 2016.
- [12] J. A. Paulson, E. A. Buehler, R. D. Braatz, and A. Mesbah, "Stochastic model predictive control with joint chance constraints," *International Journal of Control*, vol. 93, no. 1, pp. 126–139, 2020.
- [13] A. M. Jasour and B. C. Williams, "Risk contours map for risk bounded motion planning under perception uncertainties," *Robot. Sci. and Syst.*, 2019.
- [14] A. Jasour and B. Williams, "Sequential chance optimization for flow-tube based control of probabilistic nonlinear systems," *arXiv preprint arXiv:1912.03572*, 2019.
- [15] A. Wang, X. Huang, A. Jasour, and B. Williams, "Fast risk assessment for autonomous vehicles using learned models of agent futures," *Robotics: Science and Systems, to be published*, 2020.
- [16] A. M. Jasour, A. Hofmann, and B. C. Williams, "Moment-sum-of-squares approach for fast risk estimation in uncertain environments," in *2018 IEEE Conference on Decision and Control (CDC)*. IEEE, 2018, pp. 2445–2451.
- [17] N. Rhinehart, K. M. Kitani, and P. Vernaza, "R2P2: A reparameterized pushforward policy for diverse, precise generative path forecasting," in *Proceedings of the European Conference on Computer Vision (ECCV)*, 2018, pp. 772–788.
- [18] V. Witkovský, G. Wimmer, Z. Ďurišová, S. Ďuriš, and R. Palenčár, "Brief overview of methods for measurement uncertainty analysis: Gum uncertainty framework, monte carlo method, characteristic function approach," in *2017 11th International Conference on Measurement*. IEEE, 2017, pp. 35–38.
- [19] S. Frühwirth-Schnatter, *Finite mixture and Markov switching models*. Springer Science & Business Media, 2006.
- [20] M. Ono and B. C. Williams, "Iterative risk allocation: A new approach to robust model predictive control with a joint chance constraint," in *2008 47th IEEE Conference on Decision and Control*. IEEE, 2008, pp. 3427–3432.
- [21] Y. Ma, S. Vichik, and F. Borrelli, "Fast stochastic mpc with optimal risk allocation applied to building control systems," in *2012 IEEE 51st IEEE Conference on Decision and Control (CDC)*. IEEE, 2012, pp. 7559–7564.
- [22] G. M. Hoffmann, C. J. Tomlin, M. Montemerlo, and S. Thrun, "Autonomous automobile trajectory tracking for off-road driving: Controller design, experimental validation and racing," in *2007 American Control Conference*. IEEE, 2007, pp. 2296–2301.
- [23] J. Wang, J. Steiber, and B. Surampudi, "Autonomous ground vehicle control system for high-speed and safe operation," in *2008 American Control Conference*. IEEE, 2008, pp. 218–223.
- [24] P. Duchesne and P. L. De Micheaux, "Computing the distribution of quadratic forms: Further comparisons between the liu–tang–zhang approximation and exact methods," *Computational Statistics & Data Analysis*, vol. 54, no. 4, pp. 858–862, 2010.
- [25] Y. Y. Haimes and R. E. Steuer, *Research and Practice in Multiple Criteria Decision Making: Proceedings of the XIVth International Conference on Multiple Criteria Decision Making (MCDM) Charlottesville, Virginia, USA, June 8–12, 1998*. Springer Science & Business Media, 2012, vol. 487.
- [26] M. Padulo and M. D. Guenov, "Worst-case robust design optimization under distributional assumptions," *International journal for numerical methods in engineering*, vol. 88, no. 8, pp. 797–816, 2011.
- [27] D. Lam, C. Manzie, and M. C. Good, "Model predictive contouring control for biaxial systems," *IEEE Transactions on Control Systems Technology*, vol. 21, no. 2, pp. 552–559, 2012.
- [28] J. W. Peterson, "Arc length parameterization of spline curves," <https://saccade.com/writing/graphics/RE-PARAM.PDF>.
- [29] M. Floater, "Arc length estimation and the convergence of polynomial curve interpolation," *BIT Numerical Mathematics*, vol. 45, no. 4, pp. 679–694, 2005.
- [30] J. Kong, M. Pfeiffer, G. Schildbach, and F. Borrelli, "Kinematic and dynamic vehicle models for autonomous driving control design," in *2015 IEEE Intelligent Vehicles Symposium (IV)*. IEEE, 2015, pp. 1094–1099.
- [31] A. Domahidi and J. Jerez, "Forces professional. embotech gmbh (<http://embotech.com/forces-pro>)," July, 2014.
- [32] A. Zanelli, A. Domahidi, J. Jerez, and M. Morari, "Forces nlp: an efficient implementation of interior-point methods for multistage nonlinear nonconvex programs," *International Journal of Control*, vol. 93, no. 1, pp. 13–29, 2020.
- [33] J. K. Hunter, "Measure theory," *University Lecture Notes, Department of Mathematics, University of California at Davis*. [http://www.math.ucdavis.edu/~hunter/measure\\_theory](http://www.math.ucdavis.edu/~hunter/measure_theory), 2011.
- [34] K. S. Chous, "Math3060 mathematical analysis iii lecture notes," February 2013.